A simple semi-empirical photochemical model for the simulation of ozone concentration in the Seoul metropolitan area in Korea

Cheol-Hee Kim[a], Soon-Ung Park[b],*, Chang-Keun Song[b]

[a]*Department of Atmospheric Sciences, Pusan National University, Busan 609-735, Republic of Korea*
[b]*School of Earth and Environmental Sciences, Seoul National University, Seoul 151-747, Republic of Korea*

Abstract

O_3 concentrations were simulated over the Seoul metropolitan area in Korea using a simple semi-empirical reaction (SEGRS) model which consists of generic reaction set (GRS), photochemical reaction set, and the diagnostic wind field generation model. The aggregated VOC emission strength was empirically scaled by the comparison of the simulated slope of (O_3–2NO–NO_2) concentration as a function of cumulative actinic light flux against measurements on high surface ozone concentration days with the relatively weak easterly geostrophic winds at the 850 hPa level in summer when the effect of horizontal advection was fairly small. The results indicated that the spatial distribution patterns and temporal variations of spatially averaged ground-level ozone concentrations were quite well simulated compared with those of observations with the modified volatile organic compound (VOC) emission strength. The diurnal trend of the surface ozone concentration and the maximum concentration compared observations were also quite reasonably simulated. However, the maximum ozone concentration occurring time at Seoul lagged about 2 h and the ozone concentration in the suburban area was slightly overestimated in the afternoon due to the influx of high ozone concentration from the urban area. It was found that the SEGRS model could be effectively used to simulate or predict the ground-level ozone concentration reasonably well without heavy computational cost provided the emission of ozone precursors are given.
© 2005 Elsevier Ltd. All rights reserved.

Keywords: Semi-empirical photochemical model; Ozone concentration simulation; Seoul metropolitan area; Generic reaction set

1. Introduction

The Seoul metropolitan area in Korea is one of the largest metropolitan areas (population is about 22 million) in the world. The recent ozone concentration in the Seoul metropolitan area shows the increasing trend with the increase of volatile organic compound (VOC) emissions causing an emerging environmental problem in Korea. Air monitoring data in the Seoul metropolitan area over the last 10 years clearly indicate that the reported numbers of ozone warning days exceeding the National Ambient Air Quality Standards of hourly mean concentration of 120 ppb were 49, 24 and 43 days from 2000 to 2002 (NIER, 2003). As a result, various efforts have been made to develop control strategies for high O_3 concentration (Lee et al., 1998;

*Corresponding author. Tel.: +82 2 880 6715;
fax: +82 2 880 6715.

E-mail address: supark@snupbl.snu.ac.kr (S.-U. Park).

Kim and Sunwoo, 1998; Kim et al., 1998), but the modeling for the O_3 concentration over the Seoul metropolitan area is still under the developing stages.

A three-dimensional simulation model of ozone concentrations in a complex terrain area requires local-scale three-dimensional wind fields, which are usually not available. In addition, it requires detailed information on the spatial and temporal variations of emissions of disaggregated VOCs and NO_x ($NO_x = NO + NO_2$) to consider the effect of both chemical and physical processes. Therefore, the simulation of secondary air pollutions using very complicated photochemical model is hampered by the uncertainty of various input data such as emissions, meteorological fields, and initial conditions of air pollution concentrations. In addition, the complicated photochemical model requires large computing time, and possibly leads to great computational errors. Therefore, despite the continuous advancement of more sophisticated chemistry transport models in the air quality society, the simulation of ozone concentrations and day-to-day weather events remain one of the most challenging problems up to now.

The uncertainty estimation of emission inventory has been addressed in several studies (Hannah et al., 1998; Vautard et al., 2003). Most of the emission diagnostics were performed by employing the modeling and observed concentrations, but the spatial and temporal distributions of precise emission strengths still remain an open question. Over the Seoul metropolitan area, one of the major uncertainties is the lack of knowledge on the source distributions of disaggregated VOC emissions partly due to the numerous species of VOCs and their diverse source origins (US EPA, 1989). Therefore, the validation of emissions of ozone precursors has been done by comparing the modeled results obtained by scaling methods against measurements (Pierson et al., 1990; Carmichael et al., 1998; Uno et al., 1997).

Another emphasis on input data uncertainty is associated with the initial concentration fields for the simulation of secondary air pollutants over a given domain. Blond et al. (2003) described the need for the routine production of analyzed concentration maps to construct initial concentration fields. These are for observation-consistent three-dimensional quantitative maps to produce routinely analyzed fields that are required for weather forecasting. Several methods of elaborate data assimilation for providing routine air pollution concentration are recently attempted to provide initial fields of photochemical model for the prediction of ozone concentrations and to understand the photochemical process (Blond et al., 2003; Elbern and Schmidt, 2001; Vautard et al., 2001).

Azzi and Johnson (1991) have developed a very simple photochemical reaction model called the generic reaction set (GRS) to estimate the effect of a large number of VOCs and NO_x emission on ozone concentrations.
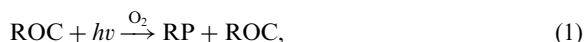
Venkatram et al. (1994) developed a systematic simplification of a detailed model and implemented it to simulate a photochemical oxidant episode in the Sab Joaquin Valley of California. The result indicated a significant improvement in the computational efficiency of the model.

In this study, we propose a very simple chemistry transport model, the Eulerian semi-empirical photochemical reaction model (semi-empirical GRS (SEGRS)) which is based on the GRS photochemical reaction set combined with a diagnostic wind model for the simulation of the ozone concentration in the Seoul metropolitan area in Korea. The required total VOC emissions are diagnosed and calibrated using the observed NO_x and ozone concentrations from measurements of monitoring networks under the weak easterly geostrophic winds at the 850 hPa level in summer that give rise to high-potential surface ozone concentration with little fluxes from the boundaries. This simple ozone concentration-simulation model is compared with other developed methods, and also discussed to provide the routine concentration map over the Seoul metropolitan area.

2. Semi-empirical photochemical reaction model

2.1. Simple photochemical reaction-GRS

The GRS scheme developed by Azzi et al. (1992) consists of the following reactions:

$$ROC + hv \xrightarrow{O_2} RP + ROC, \tag{1}$$

$$RP + NO \rightarrow NO_2, \tag{2}$$

$$NO_2 + hv \xrightarrow{O_2} NO + O_3, \tag{3}$$

$$NO + O_3 \rightarrow NO_2, \tag{4}$$

$$RP + RP \rightarrow RP, \tag{5}$$

$$RP + NO_2 \rightarrow SGN, \tag{6}$$

$$RP + NO_2 \rightarrow SNGN, \tag{7}$$

where ROC represents reactive organic compounds, RP the radical pool, SGN the stable gaseous nitrogen products, and SNGN the stable non-gaseous nitrogen products.

Eq. (1) represents all processes that lead to radical production from VOCs through photo-oxidation. Therefore, regenerated ROC has to be considered as a surrogate for all products of the oxidation of emitted VOCs. The rate constant k_1 for ROC is expressed as a function of NO_2 photolysis rate constant, weighted mean activity coefficient of the ROC and the temperature: $k_1 = \bar{a}_{ROC} k_3 f(T)$, where k_3 is the photolysis rate

constant of NO_2 and $f(T) = \exp[-4700(1/T - 1/316)]$, where T is the temperature (Azzi and Johnson, 1991).

The weighted activity coefficient $\bar{a}_{ROC}$ is determined for the mixture of ROC components from $\bar{a}_{ROC} = (\sum_{i=1}^{n} a_i C_i / \sum_{i=1}^{n} C_i)$, where n is the number of ROC components in the mixture, C_i the concentration of component i, and a_i the reactivity coefficient for component i. To determine the aggregated ROC activity coefficient we have to know the individual concentrations and reactivities of VOCs, and the weighted averaged reactivity ($E_{ROC} = \sum_{i=1}^{n} E_i a_i$) with the emission rate of VOCs (E_i) and its reactivity scaling factor (a_i).

The ROC reactivity splitting factors are calculated for six categorized hydrocarbons (alkan, alken, alkin, ethane, formaldehyde, and aromatics) which are speciated in the comprehensive Eulerian California Institute of Technology/Photochemical Airshed Model (CIT/PAM) described by McRae et al. (1982, 1983) for the applicability of several speciated VOC emissions (Kim and Park, 1999).

However, the use of categorized classes of individual VOC requires the fraction of each component that is not included in the emission source inventory. Hence, the focus of this study will be on the empirical assessment of aggregated and non-speciated total VOC emission applicable to the SEGRS model using the measurements of O_3, NO_x concentrations, and sunlight fluxes obtained from monitoring sites located over the Seoul metropolitan area.

2.2. Meteorological model

Three-dimensional diagnostic wind field model has been used to construct diurnal varying wind and turbulent fields using the hourly averaged surface observation data obtained from sites indicated in Fig. 1. The objective analysis methodology used in this study is a fast, objective, three-dimensional wind analysis in complex terrain by incorporating two important physical constraints of mass conservation and limitation of atmospheric stability on vertical displacement (Park and Kim, 1998).

The mass conserving three-dimensional wind fields in the $3 \, km \times 3 \, km$ horizontal grid spacing with 15 vertical levels (2.5, 10, 20, 50, 100, 250, 500, 750, 1000, 1250, 1500, 1750, 2000, 3000, and 5000 m) are used in the terrain following vertical coordinate. The horizontal advection is solved using a Galerkin technique with chapeau functions as finite elements (Toon et al., 1988; Park and Kim, 1998).

3. Simulations of O_3 concentration in the Seoul metropolitan area

3.1. Model domain and case selection

We consider a $75 \, km \times 63 \, km$ analysis domain, which includes city of Seoul and several satellite cities such as Incheon and Suwon (Fig. 1). The model domain is centered at $37°25'N$, $126°50'E$ with the grid of $25 \times 21 \times 15$ at a 3000 m horizontal grid spacing. Several complex terrain features dominate the domain of Seoul metropolitan area as in Fig. 1. Seoul is surrounded by mountains except to the west direction. The Yellow Sea located at the west of the model domain induces the land and sea breeze flow. Consequently, the flow field in the Seoul metropolitan area will be complicated due to the land–sea breeze and local circulation induced by complex terrains.

High-pollution potential days in summer that have been identified by the complex potential index (Jung et al., 1996) with the relatively weak easterly geostrophic winds at 850 hPa level are chosen for the simulations.

The chosen synoptic cases for this study consist of 13 days in summer (14–17, 19, 28 August 1991; 26, 27 June 1992; 5 June, 22–24 July, 22 August 1994). The common synoptic feature of chosen cases is a broad area of high pressure at 850 hPa off the southwest coast of Japan with higher insolation, weak wind, and lower relative humidity.

3.2. Emissions

The $2 \, km \times 2 \, km$ gridded NO_x and non-speciated VOC emission inventories conducted by the National Institute of Environmental Research (1994) for the reference year of 1992 over the Seoul metropolitan area are used for the simulation of ozone concentrations. Fig. 2 shows the horizontal distributions of the annual total amount of NO_x and VOC in the Seoul metropolitan area. The total emission of NO_x is mostly from line sources and thus highly dependent on traffic densities. The largest emission densities occur in the Seoul downtown area along the expressway and junctions of major roads or streets. High emissions of VOC are found at the highly populated area in the central part of Seoul because the main source of VOC is area sources emitting from the gas stations along the major roads and streets, and laundries. The annual total emission amounts of NO_x and VOC (total hydrocarbon) in 1992 are 482,083 and 112,314 $t \, yr^{-1}$, respectively. The maximum emissions of both NO_x and VOC found at around Seoul downtown are 1250 and 2510 $t \, km^{-2} \, yr^{-1}$, respectively. Also hourly emission rates of NO_x and VOC reported by Han et al. (1996) are considered in this study.

3.3. Initial and boundary conditions

As the initial and boundary conditions, the O_3 and ROC concentrations are kept to zero at the boundaries. The model simulation has been performed for 48 h with the diurnally varying diagnosed meteorological field for the chosen synoptic condition. The simulation is initiated at 01:00 LST and continued for 2 days. The first day is
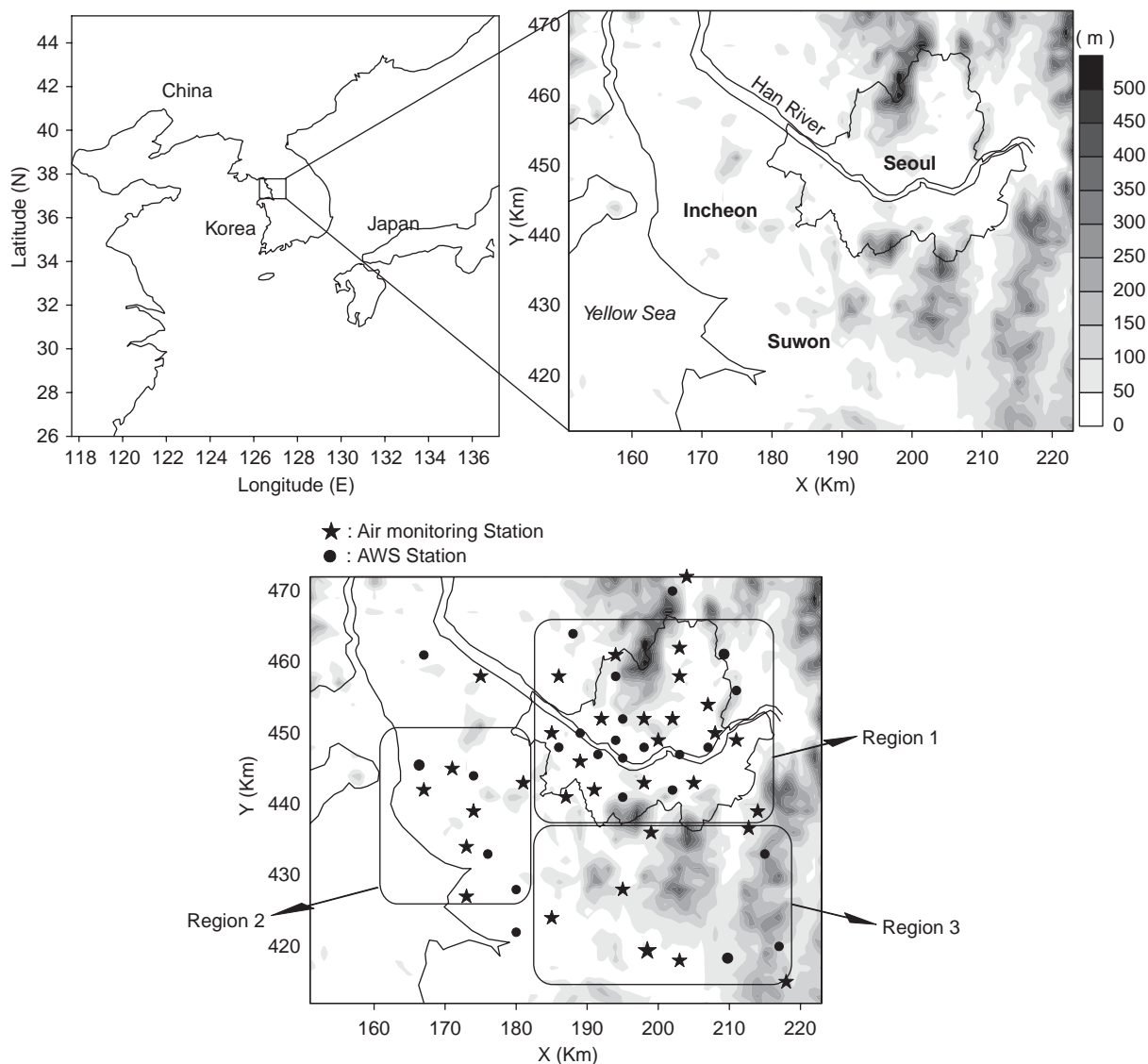
Fig. 1. The location of the Seoul metropolitan area. Topography, locations of ozone monitoring sites (●), meteorological observation stations (★), and subdivision of the model domain into three regions for the assessment of VOC emission are shown in the bottom figure.

used as a spin-up time for all species. The results of the 24-h simulation are used as initial conditions for the next 24 h simulation of the ground-level O_3 concentration.

4. Empirical approach for the assessment of aggregated VOC emission

The discrepancies between simulations and observations are generally resulting from errors underlying in the input data, such as emission inventories and meteorological data as well as model's treatment of the physical/chemical processes. One of the major uncertainties in the quantitative assessment of photosmog and oxidant formation is generally the lack of knowledge on the hydrocarbon distribution in a certain area as pointed out by earlier studies. Sources and distributions of NO_x are fairly well known (Schmid, 1993) but almost nothing is known on sources, distributions, and budget of hydrocarbon (Fabian et al., 1993).

Many previous studies reported the uncertainties associated with VOC emission inventory. For example, the roadway tunnel studies suggested that the VOC emissions might be underestimated by as much as a
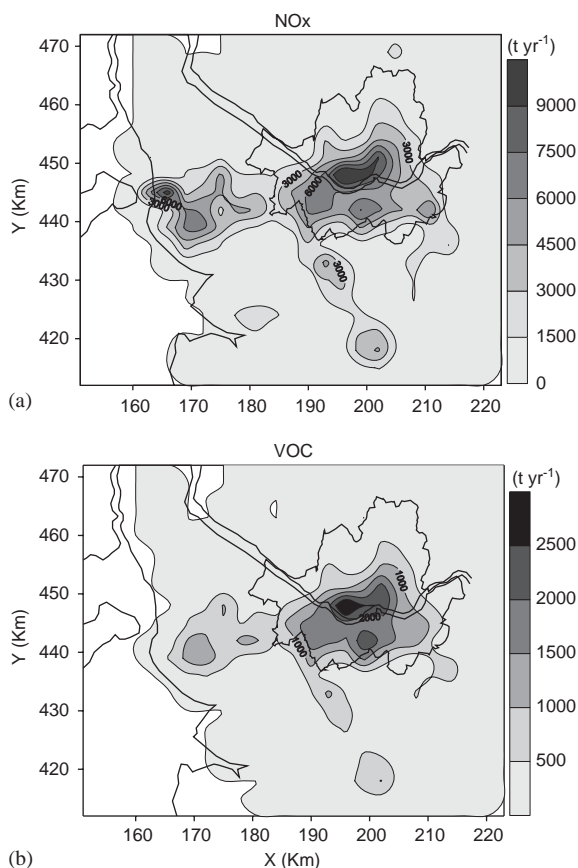
Fig. 2. Spatial distributions of annual total amount of (a) NO_x emission ($t\,km^{-2}\,yr^{-1}$) and (b) VOC emission ($t\,km^{-2}\,yr^{-1}$) in the Seoul metropolitan area.

factor of 4 (Fujita et al., 1992) and observations of motor-vehicles taken in a roadway tunnel in California added further support, showing both the absolute VOC emissions and the HC/NO_x ratios were underestimated by a factor of 3 and 4 (Pierson et al., 1990, 1996), respectively.

Thus, the prediction of the ozone concentration has been seriously hampered due to the poor VOC emission strength. Most of photochemical models employed the modified emission strengths of their precursors by comparing the results via some optimization method (Kuester and Mize, 1973) such as the empirical kinetic modeling approach (EKMA) model (US EPA, 1989) with air quality data at the monitoring sites. One empirical way of VOC emission diagnostics is to optimize VOC strength as a function of observed concentrations such as ozone and NO_x that are easily obtained from the routine monitoring network.

The assumptions of steady state ($d[RP]/dt \approx 0$) and the small concentration of RP ($[RP]^2 \approx 0$) in solving gas-phase photochemical GRS reaction in Eq (1)

(Venkatram et al., 1994) yield

$$k_1[ROC] = k_2[RP][NO] + (k_6 + k_7)[RP][NO_2]. \qquad (8)$$

Using $k_1 = \bar{a}_{ROC}k_3 f(T)$, the right-hand side of Eq. (8) becomes

$$[ROC] = \frac{1}{k_1}\frac{d[O_3 - 2NO - NO_2]}{d\int f(T)k_3 dt}. \qquad (9)$$

Eq. (9) implies that the slope of (O_3–2NO–NO_2) concentration vs. the cumulative actinic flux ($\int f(T)k_3\,dt$) obtained from the monitoring and meteorological observation sites, provides the empirical approach for the assessment of the total VOC emission.

However, the chosen synoptic condition of the weak easterly geostrophic wind will interact with the westerly sea breeze that will develop during daytime from the Yellow Sea and results in the convergence of wind fields within the metropolitan area. This may cause fluxes of pollutants from the outside of the model domain, thereby leading to errors in assessing the VOC emission using Eq. (9).

We run the SEGRS model several times in a box form according to the various factors of VOC emissions. The modeled (O_3–2NO–NO_2) concentrations vs. cumulative actinic fluxes, and the optimal slopes of the curves are fitted against observations.

Fig. 3 shows the scatter plot of the (O_3–2NO–NO_2) concentration vs. cumulative actinic flux in each region (Fig. 1) on selected days. The differences in slopes of both simulated and measured curves indicate that the surrogate VOC is approximately a factor of 4–6 times less then the observed rate (Fig. 3) suggesting that emission rates of VOC should be increased by the same factors to give much improved agreement with the observed concentration. According to the result in Fig. 3, the VOC emissions have been increased by a factor of 4 in Regions 1 and 3, and 6.5 in Region 2.

5. Result

5.1. Wind fields

Fig. 4 shows the simulated wind vectors at 10 m above the ground at 06:00, 12:00, 18:00, and 24:00 LST for the selected high-pollution potential days for the case of weak geostrophic wind (1.9 m s^{-1} from 98° direction) at 850 hPa. The easterly flows prevail over the land area during nighttime before the sunrise and the flow stagnation and down valley winds are quite well simulated in the model domain. From 09:00 LST, the easterly flows over the west coast change to westerlies which are associated with the developing sea breeze (not shown). At 12:00 LST, the westerly winds along the western coastline are intensified due to the identification of sea breezes from the Yellow Sea and penetrated inland until 18:00 LST (Fig. 4). At 24:00 LST, the sea
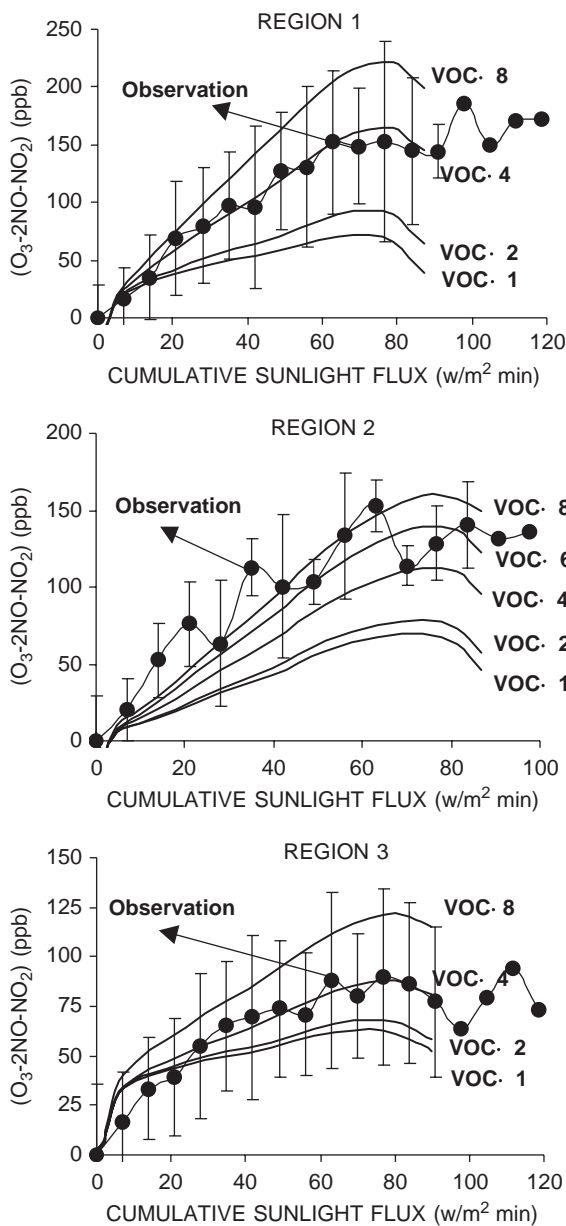
Fig. 3. Variations of observed and simulated (O_3–NO_2–2NO) concentrations with cumulative actinic flux. The simulated curves are obtained with the original VOC emission and the increased emission by a factor of 2, 4, and 8. The filled circles represent observations ± 1 standard deviation.

breezes are weakened while the down valley winds begin to develop in the sloping terrian.

5.2. Spatial distribution of O_3 concentrations

Fig. 5 shows the spatial distributions of the simulated and observed O_3 concentrations. The model simulation

indicates that precursors emitted in Seoul and Incheon are transported westward by the weak easterly winds in the morning. Thereafter, the precursors are transported eastward from Incheon due to the intensifying sea breeze resulting in the convergence of air pollutions in the eastern part of Incheon and the western part of Seoul where the maximum O_3 concentration occurs (Figs. 5b and c). The simulated maximum O_3 concentration (112 ppb) is slightly lower than that observed (126 ppb) in the analysis domain, but these simulated ozone concentration distribution patterns are fairly similar to the observed features in Figs. 5e and f. On the other hand, in the suburban area relatively higher O_3 concentrations are found in the western part of the region due to high NO_2 and VOC emission sources located along the west coastlines (Fig. 2). Higher O_3 concentrations are also found in the eastern parts of the suburban area.

Fig. 6 shows the modeled and observed diurnal variations of spatially averaged ozone concentrations in three regions shown in Fig. 1. In Region 1 (Seoul), the simulated maximum magnitude of ozone concentration is similar to the observed one, but the maximum ozone concentration occurs about 2–3 h later (Fig. 6 a). In Region 2 (Incheon), the model simulates well the peak ozone concentration although the location of predicted peak ozone concentration is shifted to the northwest where there is no monitoring site. In Region 3 (suburban area), the ozone concentration is higher than observations in the afternoon due to the transport of ozone from Seoul and Incheon (Fig. 6c), implying that the assessment and modifications of VOC emission rate are not properly taken into account due to the transboundary ozone across the region.

Statistical comparisons between the simulated and the observed O_3 concentrations are performed using the method discussed by Fox (1981). The objectively analyzed, hourly observed O_3 concentrations and the hourly simulated O_3 concentrations in the 3 km × 3 km gridded domain are used for the statistical analysis. The results of paired comparisons for hourly O_3 concentrations in Table 1 indicate no significant biases, low RMSE, and high correlation coefficients more than 0.6, suggesting good simulation capabilities of the O_3 concentration with the SEGRS model.

5.3. Discussion

In an effort to produce pollutant concentration maps with easily available inputs, many deterministic models have been developed and addressed in recent years. These models are ranging from a simple photochemical box model with not too complicated equations to complex and sophisticated chemistry transport models. The main goal of these approaches is to provide best consistency between model input and output fields so as to produce concentration maps. For the precise output
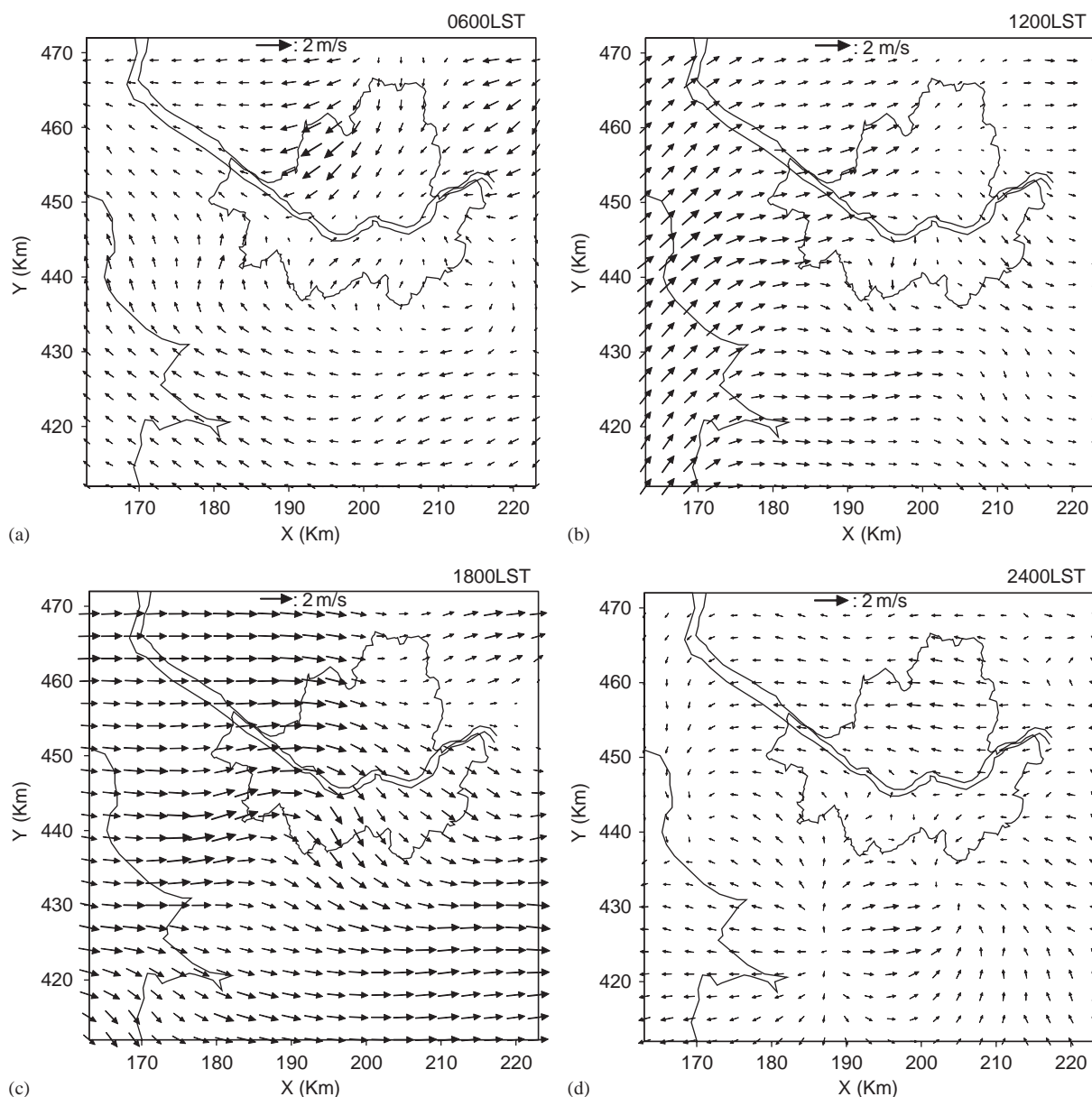
Fig. 4. Model simulated wind vectors at 10 m height above the ground at 06:00, 12:00, 18:00, and 24:00 LST.

of applied photochemical model, the assessment of emission data with a simplified or complicated chemical model has been conducted. Both simple (Jin and Demerjian, 1993) and complicated models (Sirois et al., 1999; Vautard et al., 2001) have been evaluated over a number of cases (Sirois et al., 1999), and many simplified chemistry models and data assimilation methods have been recently developed and proposed to produce routine pollutant concentration maps (Vautard et al., 2001; Elbern and Schmidt, 2001; Chang et al., 1997). In addition, effective data assimilation

techniques have been addressed in association with air quality modeling in order to generate the air pollution concentration maps (Blond et al., 2003).

The present SEGRS model with the diagnostic wind field generation model is capable of providing the ozone concentration maps in a very simple and cheap way wihout the complicated physical–chemical model that usually requires numerous accurate input data of VOC emissions, wind fields, and initial fields for various chemical components. Among them, the dominant source of uncertainty for the simulation of secondary
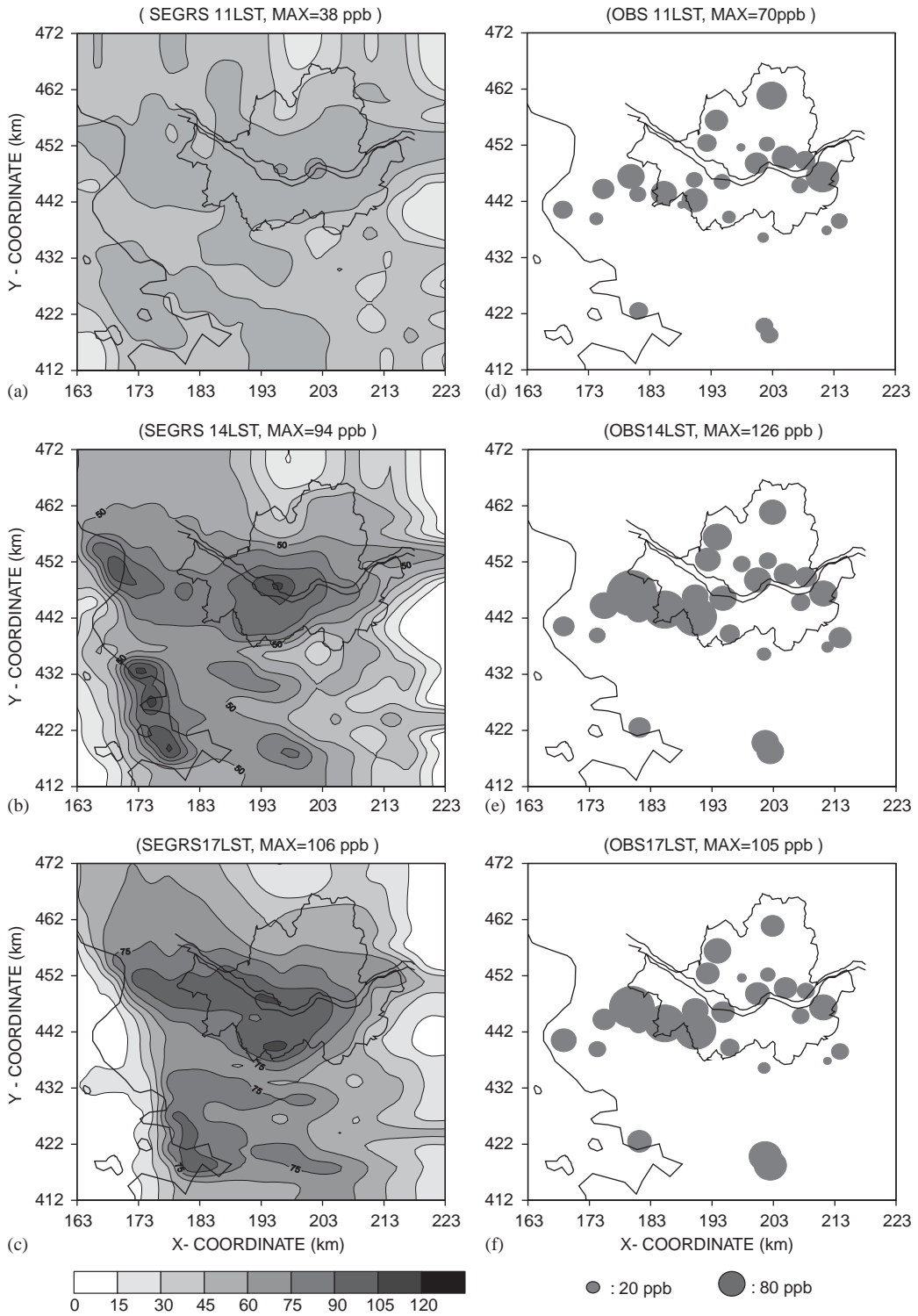
Fig. 5. Spatial distributions of simulated (left panel) and observed (right panel) ozone concentration at 11:00, 14:00, and 17:00 LST.

air quality is a lack of knowledge on the temporal and spatial distributions of emission sources. Thus, various methods of assessing the emission strength have been suggested so far (Goldan et al., 1995; Kleinman et al., 1998; Trainer et al., 2000). However, in most cases the uncertainty was found to be unable to quantify in an objective manner. Some uncertainty estimations of emission data (Hannah et al., 1998; Kuhlwein and Friedrich, 2000) indicate that the uncertainty of the individual source appears as integrating errors in the model result. A fine-tuning of sophisticated model parameters and their validation require a large computing time. Therefore, the present SEGRS model can be used as an alternative simple empirical model to produce the routine air pollutants concentration maps without heavy computational cost.
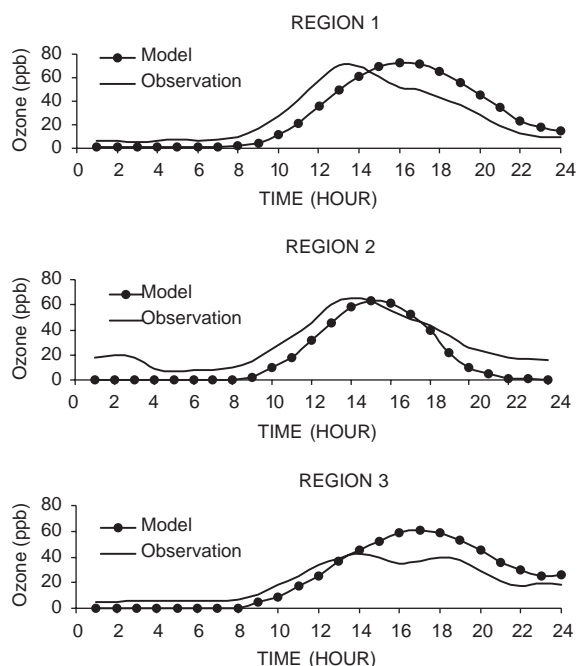
6. Summary and conclusion

The ground-level O_3 concentration has been simulated using a simple semi-empirical reaction (SEGRS) model consisting of the diagnostic wind field and simple GRS photochemical reaction over the Seoul metropolitan area for cases of high surface ozone concentration days. The required aggregated VOC emission distribution was empirically scaled by comparing the slope of $(O_3–2NO–NO_2)$ concentration against cumulative actinic light flux obtained from observations in summer with relatively weak easterly geostrophic winds at the 850 hPa level.

The simulated horizontal pattern of the surface ozone concentration was reasonably well simulated although the simulated maximum ozone concentration in Seoul

Fig. 6. Diurnal variations of the simulated and observed ozone concentration averaged in each region.

Table 1
Summary of paired comparisons for hourly ozone concentrations in various regions

	Region 1		Region 2		Region 3	
	Obs. (O)	Model (S)	Obs. (O)	Model (S)	Obs. (O)	Model (S)
Sample size	998		360		648	
Mean (ppb)	27.0	31.3	25.8	11.5	17.4	23.3
Maximum (ppb)	119.6	111.1	91.1	74.9	63.8	100.9
Standard deviation (ppb)	25.5	33.7	18.1	18.5	15.6	25.2
Correlation coefficient	0.77		0.80		0.67	
Standard deviation of (S/O)	1.65		0.37		1.04	
Mean of (S/O)	1.15		0.27		0.87	
Mean of difference (S–O)	4.27		−14.3		5.90	
Standard deviation of difference (ppb)	21.5		11.5		18.5	
Average absolute gross error (ppb)	17.0		15.6		13.2	
Root mean square error for the difference (ppb)	21.9		18.3		19.4	
Index of agreement	0.85		0.89		0.76	
Mean fractional error	0.55		1.37		0.48	
Unsystematic MSE (UMSE)	461.6		121.4		306.3	
Systematic MSE (SMSE)	18.4		216.3		73.4	
UMSE/MSE (%)	96.2		35.9		79.7	
SMSE/MSE (%)	3.8		64.1		20.1	

S: Simulated O_3 concentration. O: Observed O_3 concentration.

lagged about 2 h compared with the observation. The simulated ozone concentration in the suburban area was slightly overestimated in the afternoon mainly due to influx from the urban area. However, the results of paired comparisons for hourly O_3 concentrations for the cases show no significant biases, low RMSE, and high IOA, suggesting the good capabilities of ozone concentration simulations with the SEGRS model. It was found that the semi-empirical ozone simulation model based on GRS chemical reactions could be effectively used in simulation for generating the routine concentration map, or prediction of the ozone concentration over the Seoul metropolitan area with appropriate ozone precursor emissions.

This study mainly pertains to weak synoptic geostrophic winds to minimize influxes from the boundaries of the analysis domain. The different synoptic cases with the presently calibrated VOC emission distributions are going to be tested with the SEGRS model.

References

Azzi, M., Johnson, G.M., 1991. Notes on the generic reaction set model (GRS V 1.1). CSIRO Document, CSIRO Division of Coal and Energy Technology, New South Wales, Australia, December 1991.

Azzi, M., Johnson, G.M., Cope, M., 1992. An introduction to the genetic reaction set photochemical smog mechanism. In: Proceedings of the 11th International Clean Air Conference. 4th Regional IUAPPA Conference, Brisbane, Australia, July 1992.

Blond, N., Bel, L., Vautard, R., 2003. Three-dimensional ozone data analysis with an air quality model over the Paris area. Journal of Geophysical Research 108 2003JD003679.

Carmichael, G.R., Uno, I., Phadnis, M., Ahang, Y., Sunwoo, Y., 1998. Tropospheric ozone production and transport in the springtime in east Asia. Journal of Geophysical Research 103, 10649–10671.

Chang, M.E., Hartley, D.E., Cardelino, C., Haas-Laursen, D., Chang, W.-L., 1997. On using inverse methods for resolving emissions with large spatial inhomogeneities. Journal of Geophysical Research 102, 16023–16036.

Elbern, H., Schmidt, H., 2001. Ozone episode analysis by four-dimensional variational chemistry data assimilation. Journal of Geophysical Research 106, 3569–3590.

Fabian, P., Jakobi, G., Haustein, C., Mayer, H., Rappengluck, B., Suppan, P., 1993. Erfassung von human-biometeorologish relevanten Photooxidantien und deren Vorlaufern in einem Ballungsraum. GSF-Bericht 31/93, 57-73, GSF- Forschungs-zentrum fur Umwelt und Gesundheit, Neuherberg.

Fox, D.G., 1981. Judging air quality model performance. Bulletin of American Meteorological Society 62, 599–609.

Fujita, E.M., Croes, B.E., Bennett, C.L., Lawson, D.R., Lurmann, F.W., Main, H.H., 1992. Comparison of emission and ambient concentration ratios of CO, NO_x, and NMOG in California's South Coast Air Basin. Journal of the Air and Waste Management Association 42, 264–276.

Goldan, P.D., Trainer, M., Kuster, W.C., Parrish, D.D., Carpenter, J., Roberts, J.M., Yee, J.E., Fehsenfeld, F.C., 1995. Measurements of hydrocarbons, oxygenated hydrocarbons, carbon monoxide, and nitrogen oxides in an urban basin in Colorado: implications for emission inventories. Journal of Geophysical Research 100, 22771–22783.

Han, J.-S., Kim, B.-G., Kim, S.-D., 1996. Ozone simulation and sensitivity test under varying emission condition. Journal of Korean Society of Environmental Impact Assessment 5 (1), 69–77.

Hannah, S.R., Chang, J.C., Fernau, M.E., 1998. Monte Carlo estimates of uncertainties in predictions by a photochemical grid model (UAM-IV) due to uncertainties in input variables. Atmospheric Environment 32, 3619–3628.

Jin, S., Demerjian, K., 1993. A photochemical box model for urban air quality study. Atmospheric Environment 27B, 371–387.

Jung, Y.-S., Park, S.-U., Yoon, I.-H., 1996. Characteristic features of local air quality associated with meteorological conditions. Journal of Korean Meteorological Society 32 (2), 271–290 (in Korean).

Kim, C.-H., Park, S.-U., 1999. The development and application of semi-empirical photochemical reaction model. Journal of Korean Meteorological Society 35 (3), 421–431 (in Korean).

Kim, J.Y., Ghim, Y.S., Kim Y.P., 1998. Photochemical modeling of July 1994 ozone episode in the metropolitan Seoul area. Proceedings of the 91st Annual Meeting and Exhibition, Air and Waste Management Association, San Diego, CA, 14-18 June, 98-WPD.03P.

Kim, K.J., Sunwoo, Y., 1998. A study on the reduction of ozone concentration in the metropolitan area. Spring meeting of the Korea Air Pollution Research Association, Seoul Korea, 8-9 May, D-1 (in Korean)

Kleinman, L.I., Daum, P.H., Imre, D.G., Cardelino, C., Olszyna, K.J., Zika, R.G., 1998. Trace gas concentrations and emissions in downtown Nashville during the 995 southern oxidants study/Nashville intensive. Journal of Geophysical Research 103, 22545–22553.

Kuester, J.L., Mize, J.H., 1973. Optimization Techniques with Fortran. McGraw-Hill, New York, NY.

Kuhlwein, J., Friedrich, R., 2000. Uncertainties of modeling emissions from road transport. Atmospheric Environment 34, 4603–4610.

Lee, C.B., Choi, J.H., Kim, Y.K., 1998. Simulation of an ozone episode in the Seoul metropolitan area in June using the urban airshed model. Spring meeting of the Korea Air Pollution Research Association, Seoul Korea, 8–9 May, B-3 (in Korean).

McRae, G.J., Goodin, W.R., Seinfeld, J.H., 1982. Development of a second-generation mathematical model for urban air pollution—I. Model formulation. Atmospheric Environment 16, 679–696.

McRae, G.J., Goodin, W.R., Seinfeld, J.H., 1983. Development of a second-generation mathematical model for urban air pollution—II. Evaluation of model performance. Atmospheric Environment 17, 501–522.

NIER (National Institute of Environmental Research), 1994. Study on visibility and smog phenomena in Seoul Metropolitan area. NIER Report No. 94-27-442, 158pp (in Korean).

NIER (National Institute of Environmental Research), 2003. Annual Report of air quality in Korea. Kyongseo-dong, Seo-gu Inc., Korea, pp. 404–170 (in Korean).

Park, S.-U., Kim, C.-H., 1998. A numerical model for the simulation of SO2 concentrations in the Kyongin region Korea. Atmospheric Environment 33, 3119–3132.

Pierson, W.R., Gertler, A.W., Bradow, R.L., 1990. Comparison of the SCAQS tunnel study with other on road vehicle emission data. Journal of the Air and Waste Management Association 40, 1495–1504.

Pierson, W.R., Gertler, A.W., Robinson, N.F., Sagebiel, J.C., Zielinska, B., Bishop, G.A., Stedman, D.H., Zweidinger, R.B., Ray, W.D., 1996. Real-world automotive emissions—summary of studies in the Fort McHenry and Tuscarora Mountain tunnels. Atmospheric Environment 30, 2233–2256.

Schmid, S., 1993. An estimation of the average NO_x contamination of Southern Bavaria by regional emitters. Theoretical and Applied Climatology 47, 33–50.

Sirois, A., Pudyklewicz, J.A., Kallaur, A., 1999. A comparison between simulated and observed ozone mixing ratios in eastern North America. Journal of Geophysical Research 104, 21397–21423.

Toon, O.B., Turco, R.P., Westphal, D., Malone, R., Liu, M.S., 1988. A multidimensional model for aerosols : description of computational analogs. Journal of Atmospheric Science 45, 2123–2143.

Trainer, M., Parrish, D.D., Goldan, P.D., Roberts, J., Fehsenfeld, F.C., 2000. Review of observation-based analysis of the regional factors influencing ozone concentrations. Atmospheric Environment 34, 2045–2061.

Uno, I., Wakamatsu, S., Ueda, H., Murano, K., Sakamaki, S., Kurita, H., Satsumabayshi, H., Horai, S., 1997. Behavior of secondary pollutants and volcanic SO_2 over Kyushu during a spring high pressure system. Journal of Japanese Society of Atmospheric Environment 32, 404–424.

US EPA (US Environmental Protection Agency), 1989. Procedures for applying city-specific EKMA. EPA-450/4-89-012, Research Triangle Park, NC.

Vautard, R., Beekmann, M., Roux, J., Gombert, D., 2001. Validation of a hybrid forecasting system for the ozone concentrations over the Paris area. Atmospheric Environment 35, 2449–2461.

Vautard, R., Martin, D., Beekmann, M., Drobinski, P., Friedrich, R., Jaubertie, A., Kley, D., Lattuati, M., Moral, P., Neininger, B., Theloke, J., 2003. Paris emission inventory diagnostics from ESQUIF airborne measurements and a chemistry transport model. Journal of Geophysical Research 108 2002JD002797.

Venkatram, A., Karamchandani, P., Pai, P., Goldstein, R., 1994. The development and application of simplified ozone modeling system (SOMS). Atmospheric Environment 28, 3665–3678.